

The Role of Adsorbed Water on Adhesion Force of Powder Particles

Masatoshi Chikazawa*, Takafumi Kanazawa*
and Toshihide Yamaguchi*

Department of Industrial Chemistry
Tokyo Metropolitan University

Abstract

Adhesion forces generated at a contact point between spherical and plate specimens of potassium halides, commercial soda-lime glass and Pyrex glass were estimated by using an electrobalance, and adsorption isotherms of water vapor and methyl alcohol on these samples were also measured. The thickness of a liquid bridge and the pressure at which a capillary condensation occurs for the first time have been investigated using porous glasses each of which has a monodispersed pore radius. The following conclusions have been deduced from the comprehensive comparison of the obtained results. The adhesion forces under low and high water vapor pressures are suggested to be ascribed to hydrogen bond and liquid bridge, respectively. A marked increase of adhesion force observed in the pressure range $0.6 < P/P_0 < 0.85$ is due to a transformation from hydrogen bond to liquid bridge and due to a change in the physical property of condensed liquid. The thickness of the liquid bridge at $P/P_0 = 0.6$ is presumed to be $29\text{-}37\text{\AA}$

1. Introduction

The powder characteristics, i.e. angle of repose, properties of packing and friction, and fluidity, are largely influenced by adhesion forces generated among powder particles. Therefore, during storage, flow and handling of powders, the adhesion forces very often cause severe problems. As a rule, these adhesion forces are classified into five major groups such as solid bridges, adhesion and cohesion forces in not freely movable binders, interfacial forces and capillary pressure at freely movable liquid surfaces, attraction forces between solid particles, and interlocking bonds¹⁾. In cases of hydrophilic powders the adhesion force due to water vapor adsorption is generally regarded to be larger than the van der Waals force, and becomes an origine of troublesome matters in handling powders under atmosphere. The force produced by water adsorption also closely relates to the

physical property of water layer, and its property varies with the thickness of water layer formed on a solid surface. However, the informations concerning the following three points, 1) the relationship between the thickness of water film formed on a solid surface and humidity of atmosphere around the sample, 2) the changes in physical properties of the water film with its thickness, 3) the thickness of a liquid bridge formed at the neighborhood of a contact point between two sample particles, are scarcely obtained. The purpose of the present study is to clarify the generation mechanism of the adhesion force due to water vapor adsorption, by discussing the above obscure points.

2. Experimental

2.1 Materials

The samples used were alkali halides (i.e. KCl and KBr), commercial soda-lime glass beads (7-20 mesh), Pyrex glass and porous glass. Alkali halides were purified by two times recrystallization in their aqueous solutions.

* Fukasawa, Setagaya-ku, Tokyo, 158
TEL. 03 (717) 0111

Received June 26, 1984

The samples for adhesion force measurement

A spherical sample of the alkali halide was prepared by covering a glass bead with the alkali halide itself as follows. A glass bead with 2-3 mm in diameter was dipped for a moment in a melted alkali halide under an atmosphere of nitrogen. In case of Pyrex glass, a spherical sample was obtained by fusing an end of its fibriform glass using a gas burner. The commercial soda-lime glass bead was used without any treatment. On the other hand, a sheet specimen of an alkali halide was made by pressing the powder sample. In case of Pyrex glass, a commercially available glass sheet was used. The commercial soda-lime glass was melted and made in a sheet-form.

The samples for adsorption measurement

A solution, 100 ml 20-30 wt%, of a purified alkali halide sample was poured in five-fold volume of ethyl alcohol cooled to $-80 \sim -90^\circ\text{C}$ with stirring. A precipitate obtained was filtered, washed four times with absolute ethyl alcohol, and then evacuated under a reduced pressure of 10^{-6} mmHg. The specific surface areas of KCl and KBr samples were found to be 1.04 and 0.71 m^2/g , respectively. For Pyrex glass, the powder samples which had large surface areas (0.2-0.4 m^2/g) were prepared by grinding hollow Pyrex capillaries and slender Pyrex rods. The porous glass sample (Thirsty Glass Corning Code 7930, 200 m^2/g) having a monodispersed pore radius of 20 Å was treated with 0.1% HF aqueous solution for a proper duration to widen the pore radius. The resulted pore radii were calculated to be 27, 30 and 33 Å from nitrogen adsorption measurements.

2. 2 Adhesion force measurement

Adhesion forces generated at a contact point between spherical and sheet specimens made of the same material were measured by using an electrobalance under various water vapor pressures. In cases of alkali halides, a caking due to water vapor adsorption occurred at high water vapor pressure, and the adhesion force suddenly increased with the strength of the caking. However, the effect of the caking on the adhesion force was unrecognized within 20 minutes since the two specimens were in contact

with each other. Therefore, the adhesion force was measured after the lapse of 5-15 minutes and 5-10 times measurements were carried out for accuracy.

2. 3 Adsorption isotherms

The adsorption isotherms of nitrogen, water and methyl alcohol vapor on the samples were determined volumetrically by using an adsorption apparatus. When the vapor pressure of an adsorbate unchanged for 15 minutes, adsorption equilibrium was regarded to be established. The equilibrium pressures of water and methyl alcohol were measured using a mercury manometer and a reading magnifier having a resolution of 10^{-2} mmHg. The effects of a tube radius of the manometer and a shape of its meniscus on the measured pressure were considered and the equilibrium pressures were corrected.

3. Results and discussion

3. 1 Adhesion force

Generally, in cases of the powder particles whose surfaces have a hydrophilic property, it is known that the adhesion force due to water vapor adsorption increases abruptly above the pressure of about 60%rH and has a maximum value in a high pressure region of 70-90%rH²). However, no detailed informations concerning

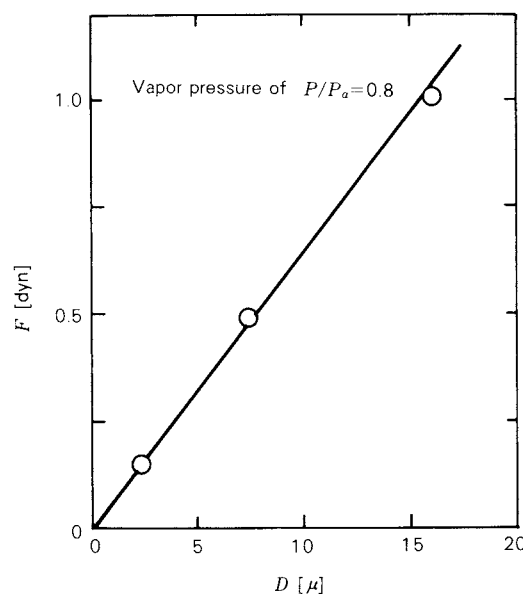


Fig. 1 Relationship between adhesion force and particle size at water vapor pressure of $P/P_0 = 0.8$

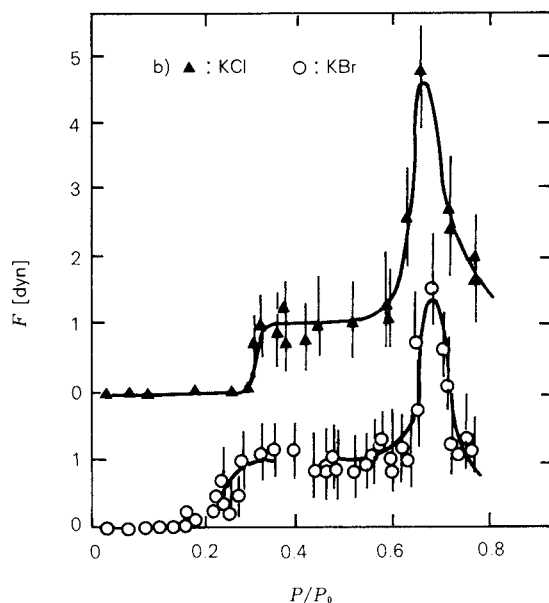
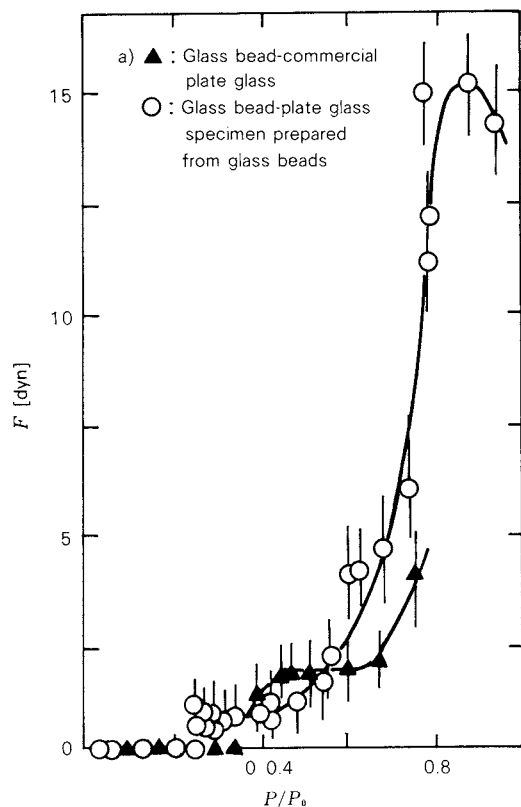


Fig. 2 Changes in adhesion forces of potassium halides at a contact point with water vapor pressure

the mechanism of such adhesion force change are obtained. According to theoretical calculations, the adhesion force generated by a liquid bridge which is formed in a gap of the separated two spherical particles³⁾ or made at a contact point between a projection of conical

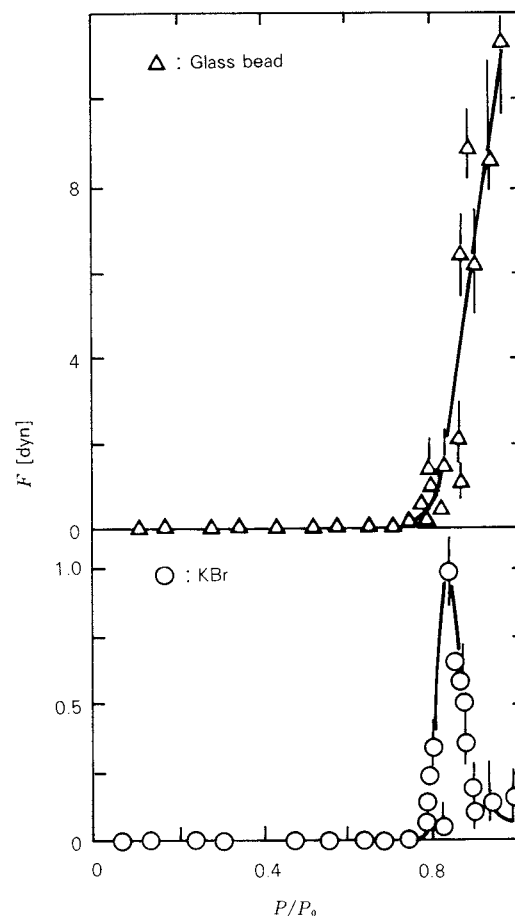


Fig. 3 Changes in adhesion forces of glass bead, and KBr with methyl alcohol vapor pressure

shape and a sheet or spherical specimen⁴⁾, increases with the amount of absorbed water. As for the former mechanism, a maximum value of the adhesion force arises in further adsorption, but in the latter case it is not observed. The effect of particle size on the adhesion force is shown in Fig. 1⁵⁾. The adhesion force increased linearly with the radius of a spherical particle. Hereafter, a spherical sample with a proper size was used. In Fig. 2 changes in the adhesion force with increase of water vapor pressure are given⁶⁾. For KBr sample, the adhesion force was detected above the pressure of $P/P_0 = 0.20$, and was roughly constant in the range of $0.2 < P/P_0 < 0.55$. At the pressure larger than $P/P_0 = 0.6$ the force increased suddenly, and then decreased markedly with increase of the pressure in the range above $P/P_0 = 0.66$. As for KCl sample, a similar phenomenon was observed. The water vapor pressure at which the adhesion force began to appear was

slightly higher than that of KBr. In cases of the glass beads, the same type of adhesion force curves were observed. From these results, the effect of varying the samples on the characteristics of the adhesion curve seems to be small.

In Fig. 3 changes in adhesion force with increase of methyl alcohol vapor pressure are shown⁷⁾. The force was recognized only above the pressure of $P/P_0 = 0.8$ and it disappeared in the lower pressure region. On the other hand, in case of water adsorption the adhesion force appeared even in the low pressure region. Such discrepancy in shape of the adhesion force curve is explained in terms of the adhesion force generated by hydrogen bond. In case of water adsorption, three dimensional hydrogen bond formation will be possible, whereas it will be difficult in case of methyl alcohol adsorption on account of the difference of molecular structure between the two molecules. A detailed discussion concerning the hydrogen bond formation will be made in the following section.

3. 2 Adsorption isotherms

Adsorption isotherms of water vapor and methyl alcohol on various samples are shown in Fig. 4⁸⁾. In the vicinity of $P/P_0 = 0.2$ at which the adhesion force was measured for the first time, the coverage $\theta = S_{\text{H}_2\text{O}}/S_{\text{N}_2}$ of KBr surface with water molecules was found to be 0.58, assuming the cross-sectional area of 10.5 \AA^2 for a water molecule, where $S_{\text{H}_2\text{O}}$ and S_{N_2} are surface areas determined from water vapor and nitrogen adsorptions, respectively. For KCl sample, the coverage $\theta = 0.50$ estimated at the appearance of the force was slightly smaller than that of KBr. On the other hand, regarding the glass samples the coverages necessary for generating the force were obtained to be $\theta < 1.5$. In these cases the accurate coverages were not obtained on account of the presence of micropores or migration of water molecules into the glass samples. As for the alkali halides, the adhesion force was generated in spite of the small amount of adsorbed water. Moreover, the capillary condensation is considered to be difficult at a contact point since about 40-50% of the alkali halides surfaces are bare. Therefore, the formation of a liquid bridge is concluded to be impossible. From these results the other generation mechanism of adhesion force such

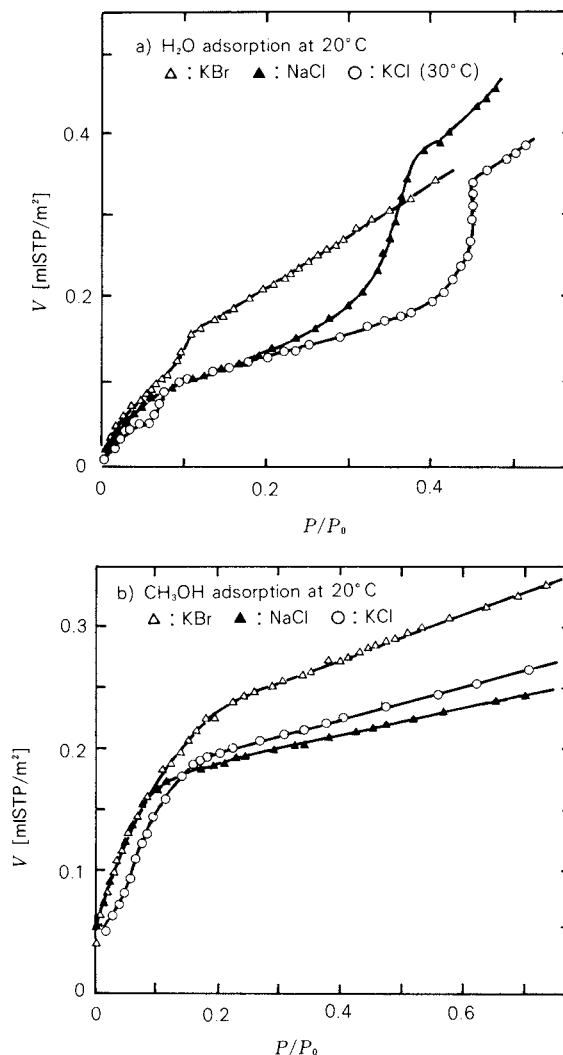


Fig. 4 Adsorption isotherms of H₂O and CH₃OH on alkali halides

as hydrogen bond must be proposed. For KCl sample, changes in adhesion force with the amounts of water and methyl alcohol are given in Fig. 5⁷⁾. In case of the water adsorption the force was detected at low coverages $0.5 < \theta < 1.5$, while the force was undetected at the same coverages in methyl alcohol adsorption. Considering these results, the difficulty of the three dimensional hydrogen bond formation will be reasonable in methyl alcohol adsorption.

The isosteric heats of methyl alcohol adsorption on KCl, NaCl and KBr are given in Fig. 6⁸⁾. In cases of KCl and NaCl samples, clear auto-phobic adsorptions were inferred since the isosteric heats of adsorption decreased markedly after the completions of their monolayer adsorptions. The similar phenomena are ob-

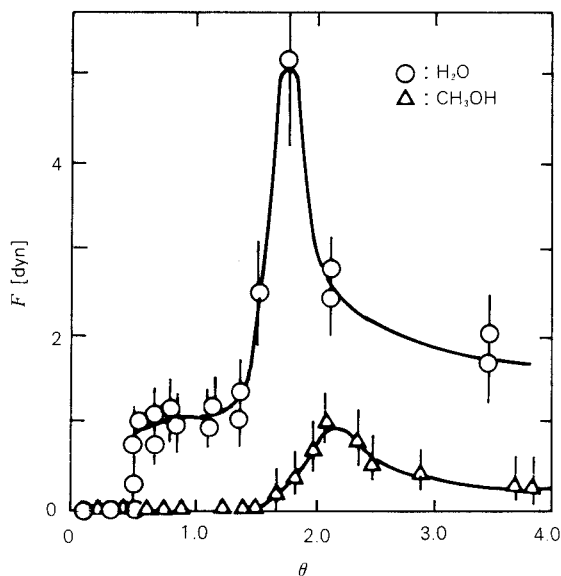


Fig. 5 Changes in adhesion forces of KCl with adsorbed amounts of water and methyl alcohol

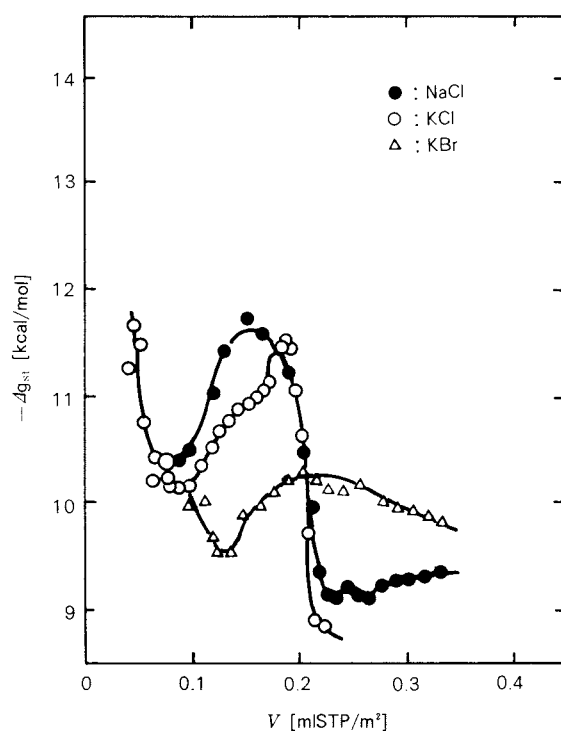


Fig. 6 Isosteric heats of adsorption of methyl alcohol on alkali halides

served for the other adsorbates⁹⁾. These facts imply that a polar group in a methyl alcohol molecule is located under its methyl group, and an interaction between a methyl alcohol molecule and the polar groups in formerly adsorbed molecules is difficult.

3. 3 Thickness of a liquid bridge

Detailed informations about the following two points, 1) the water vapor pressure at which a capillary condensation can occur and form a liquid bridge at a contact point for the first time and 2) the thickness of the liquid bridge, are not obtained yet. The adsorption isotherms of water vapor on Pyrex glass particles prepared by grinding hollow Pyrex capillaries and slender Pyrex rods are given in Fig. 7⁵⁾. The former sample is supposed to contain a great number of micropores having various pore radii. The adsorptive properties of these two samples are necessarily equal each other as the samples consist of the same components. Therefore, if the adsorbed amounts of water vapor per unit surface area estimated from nitrogen adsorption are plotted against the pressure, the two adsorption isotherms will coincide. In a pressure range $0 < P/P_0 < 0.6$, the expected coincidence was recognized. However, a discrepancy between the two isotherms were observed above the pressure of $P/P_0 = 0.6$. As the adsorbed amounts of water vapor for the sample prepared by grinding hollow Pyrex capillaries are greater than those for the another sample, a capillary condensation is considered to occur at the pressure of $P/P_0 = 0.6$ for the first time in some scale. Hence, a liquid bridge which generates the adhesion force is supposed to be formed by capillary condensation at the pressure above $P/P_0 = 0.6$. Using the Kelvin equation (1) and assuming the cylindrical pore shape, the pore radius (r_p) of the capillary is calculated to be 37\AA . This value is obtained by adding a value of multilayer thickness (t) to the Kelvin radius (r_k).

$$r_k = - \frac{2V\gamma \cos\alpha}{RT \ln P/P_0} \quad (1)$$

$$r_p = t + r_k \quad (2)$$

Where P and P_0 values are vapor pressures of adsorption equilibrium and bulk liquid at measurement temperature, respectively, and α represents a contact angle of liquid film. The values V and γ are molar volume and surface tension of the liquid condensed in a micropore. The shape of a liquid bridge formed at a contact point between the two samples is regarded approximately as a thin disk. From these results, the thickness of the liquid bridge is con-

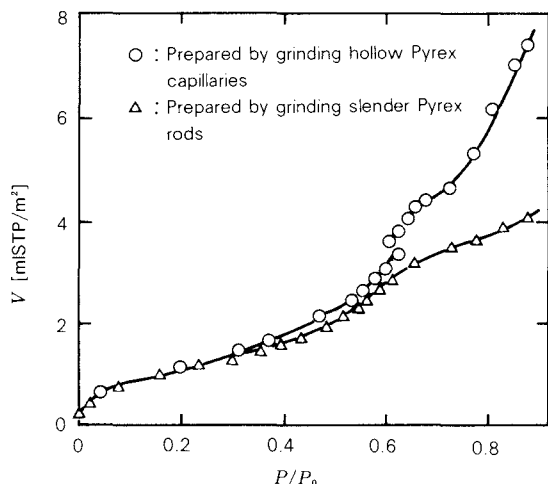


Fig. 7 Adsorption isotherms of water vapor on Pyrex glass particles at 20°C

cluded to be 37Å.

In order to obtain some further informations about the thickness of a liquid bridge, the porous glass with a monodispersed pore radius distribution (20Å) was used and the capillary condensation phenomenon was studied varying its pore radius distribution. The adsorption and desorption isotherms of nitrogen, water vapor and methyl alcohol on porous glass sample (20Å) are shown in Fig. 8⁵⁾. The pore radius distributions estimated from these desorption

isotherms are also illustrated in Fig. 8⁵⁾. A monodispersed distribution was obtained for each adsorbate. However, the discrepancy in the peak value of the distribution was recognized in spite of using the same sample. As the thickness (t) of multilayer is evaluated accurately from an adsorption isotherm, such discrepancy will be ascribed to the Kelvin radius (r_k). The r_k value is calculated based on the following three assumptions, 1) the contact angle (α) of the liquid film formed on a solid surface is zero, 2) the molar volume (V) of condensed liquid in a micropore is equal to that of bulk liquid, and 3) the surface tension (γ) of the liquid film is the same as that of bulk liquid. In a desorption process, the actual contact angle of the liquid film is considered to be zero since the angle is regarded as a receding contact angle. Moreover the molar volume of condensed liquid in a micropore is presumed to be approximately equal to that of bulk liquid¹⁰⁾. From these results, the discrepancy in the pore radius estimation will be mainly due to the change in the surface tension of the liquid condensed in a micropore. The surface tension of the condensed liquid can be determined so as to obtain the correct pore radius distribution calculated from nitrogen desorption. The influence of the pore radius on the

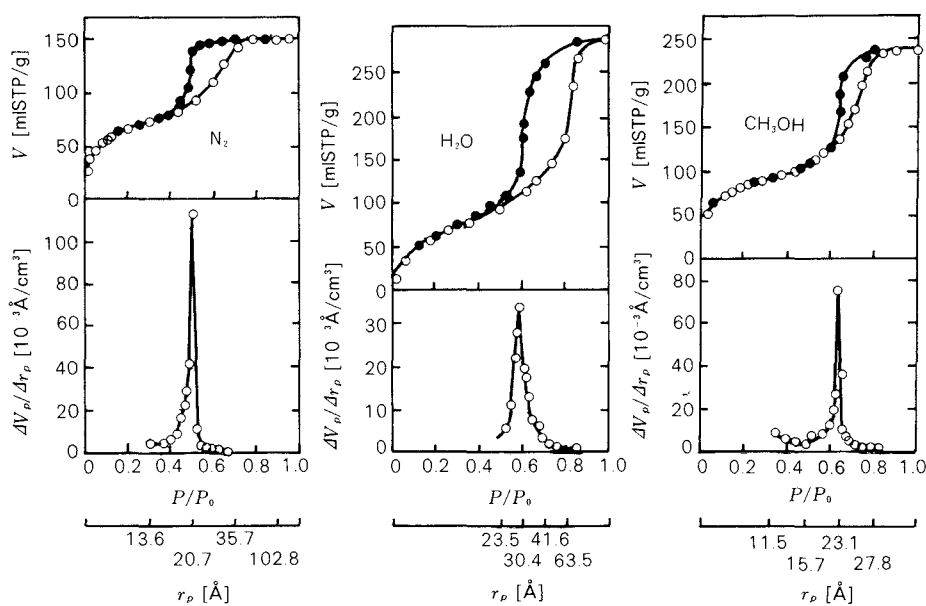


Fig. 8 Adsorption and desorption isotherms of N₂, H₂O and CH₃OH on porous glass, and pore size distributions calculated from their desorption isotherms

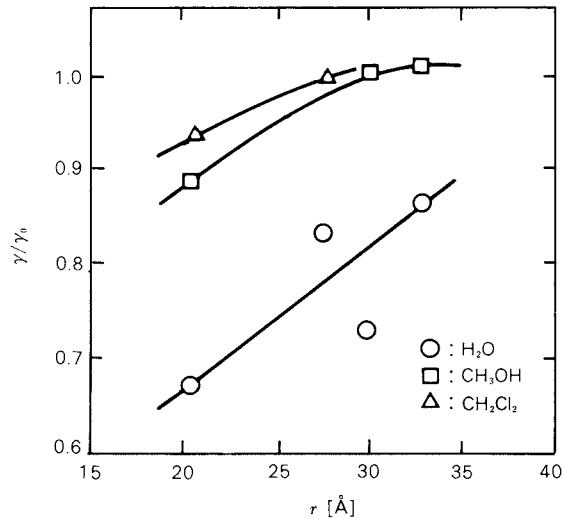


Fig. 9 Effect of solid surface on surface tension of condensed liquid

surface tension of the condensed liquid are shown in Fig. 9⁷⁾. The surface tension became large with increase of the pore radius and then equalled that of bulk liquid. The greatest change in the surface tension was observed in water vapor adsorption. This phenomenon is explained that the influence of a solid surface on the liquid structure of water layer extends to further distance comparing the other adsorbates on account of the ability of three dimensional hydrogen bond formation. As for water molecules, such affected region is presumed to be about 40 \AA . Considering the change in surface tension of the condensed liquid, the thickness of a liquid bridge is revaluated to be about 29 \AA at $P/P_0 = 0.6$. Hence, the thickness of a liquid bridge is concluded to be in the range from 29 \AA to 37 \AA at the pressure of $P/P_0 = 0.6$.

3. 4 Phase transition temperature

It is shown in the above section that the physical properties of the liquid condensed in a micropore are different from those of bulk liquid. In this section, these physical property changes are discussed again from a different angle such as variation of phase transition temperature. The relationship between measurement temperatures and water vapor pressures in adsorption equilibrium, i.e. the Clausius-Clapeyron plot, is given in Fig. 10. An intersection of two linear lines was observed. The isosteric heat of water vapor adsorption can be

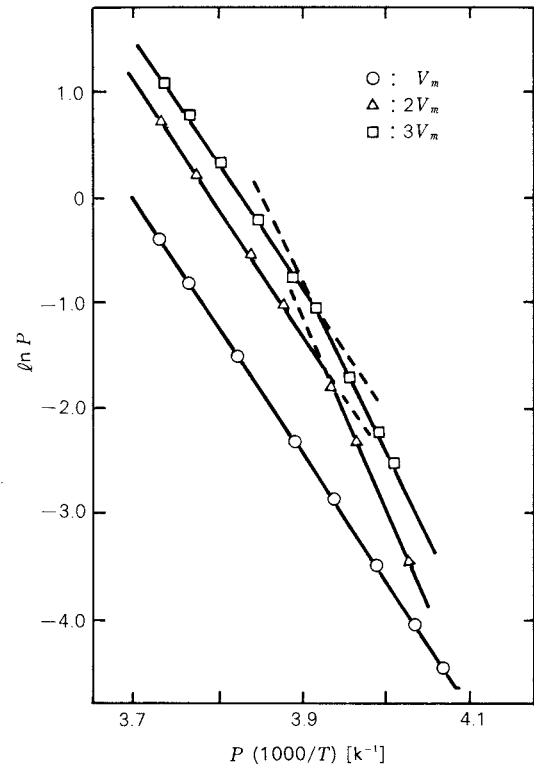


Fig. 10 Clausius-Clapeyron plots of water vapor adsorption on porous glass

estimated from an incline of the linear line. The value determined from the linear part of the high temperature region equalled approximately the liquefaction heat of water vapor. On the other hand, the heat evaluated from the low temperature region corresponded to the sublimation heat of bulk ice. Therefore, the temperature at the intersection is considered to represent a phase transition temperature of the adsorbed water layer. The obtained temperature is lower than the melting point of bulk ice since the liquid structure of the water layer is different from that of bulk water. The changes in the transition temperature with the adsorbed amount of water are given in Fig. 11⁷⁾. The temperature variation tendency with the adsorbed amount was slightly different each other. However, the abrupt increase of the transition temperature was recognized in the adsorbed range about $2 < V/V_m < 3$, where V_m represents a monolayer capacity and V is the adsorbed amount. This experimental result shows that the liquid structure of the water layer changes markedly in the same range. On the other hand, a completion of $2-3V_m$ adsorption was observed at the pressure of $0.6 <$

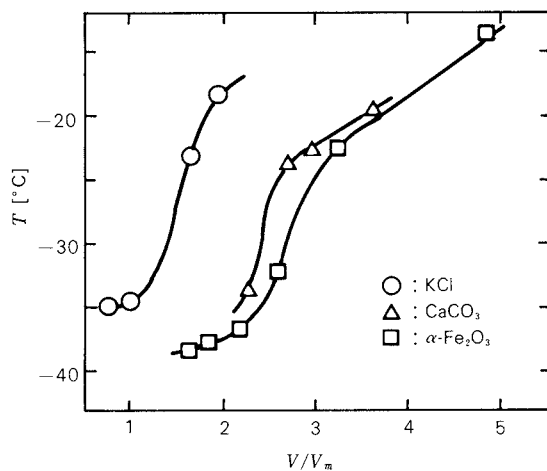


Fig. 11 Phase transition temperature of water layer formed on solid surfaces

$P/P_0 < 0.8$. In the same pressure range, the capillary condensation occurred in a micro space and the adhesion force due to the formation of a liquid bridge arose. From these results it is concluded that the abrupt increase of the adhesion force is due to the change in the generation mechanism of the force, such as from hydrogen bond to liquid bridge, and due to the variation of the surface tension of a liquid bridge.

For KCl sample no phase transition was observed at adsorbed amount below $0.18 \text{ m}\ell \text{ STP}/\text{m}^2$ corresponding to the coverage of 0.54. The obtained result indicates that water molecules are adsorbed in a dispersed state and do not form a cluster which causes a phase transition. However, the adhesion force was detected in such a condition. Therefore, the force generated in low pressure region is considered to be ascribed to the formation of hydrogen bond. This conclusion is in accord with the description in the foregoing section.

4. Conclusion

Adhesion forces generated at a contact point between spherical and plate specimens of various samples were measured by using an electrobalance, and adsorption isotherms of water vapor and methyl alcohol for those samples were also determined. Moreover, capillary condensation phenomena have been investigated in order to clarify the physical property changes

of the water layer formed on a solid surface. The following results have been obtained.

- 1) The adhesion force generated at water vapor pressure below $P/P_0 = 0.6$ is presumed to be ascribed to the formation of hydrogen bonds. As the physical properties of water layer are different from those of bulk water, a capillary condensation which forms a liquid bridge is difficult.
- 2) A marked increase of adhesion force in high pressure region $0.6 < P/P_0 < 0.8-0.9$ is explained in terms of the change in adhesion mechanism from hydrogen bond to liquid bridge, and in the same range the physical properties, i.e. surface tension and phase transition temperature, of condensed liquid vary with the thickness of water layer.
- 3) The surface tension of the water condensed in a micropore (pore radius 20\AA) at the pressure of $P/P_0 = 0.6$ was estimated to be about 68% of bulk water.
- 4) A capillary condensation occurs only above the pressure of $P/P_0 = 0.6$ and the thickness of the liquid bridge at $P/P_0 = 0.6$ is considered to be $29-37\text{\AA}$.

References

- 1) Pietsh W.B.: *Trans. ASME*, **B81**, 435 (1969).
- 2) Asakawa S. and G. Jimbo: *J. Soc. Materials Sci., Japan*, **16**, 358 (1967).
- 3) Pietsch H. and H. Rumpf: *Chem. Ing. Tech.*, **39**, 885 (1967).
- 4) K. Iinoya and H. Muramoto: *J. Soc. Materials Sci., Japan*, **16**, 352 (1967).
- 5) Yamaguchi T., M. Tomita, M. Chikazawa and T. Kanazawa: *J. Soc. Powder Technol., Japan*, **16**, 514 (1979).
- 6) Chikazawa M., W. Nakajima and T. Kanazawa: *J. Soc. Powder Technol., Japan*, **14**, 18 (1977).
- 7) Chikazawa M., T. Yamaguchi and T. Kanazawa: "Proceeding of International Symposium on Powder Technology" p.202, (1982) The Soc. Powder Technology.
- 8) Chikazawa M. and T. Kanazawa: *Bull. Chem. Soc. Japan*, **50**, 2837 (1977).
- 9) Barto J., J.L. Durham, V.F. Baston and W.H. Wade: *J. Colloid Interface Sci.*, **22**, 491 (1966).
- 10) H.L. McDermot and W.G.M. Tuck: *Can. J. Res.*, **28B**, 292 (1950).